Published in final edited form as:
Cancer Res. 2012 October 1; 72(19): . doi:10.1158/0008-5472.CAN-12-1248.

Hedgehog Signaling Is a Novel Therapeutic Target in Tamoxifen-Resistant Breast Cancer Aberrantly Activated by PI3K/AKT Pathway

Bhuvaneswari Ramaswamy[#1,5], **Yuanzhi Lu**[#2], **Kun-yu Teng**[2], **Gerard Nuovo**[3], **Xiaobai Li**[4], **Charles L. Shapiro**[1,5], and **Sarmila Majumder**[2,5]

[1]Division of Medical Oncology, The Ohio State University, Columbus, Ohio

[2]Department of Molecular and Cellular Biochemistry, The Ohio State University, Columbus, Ohio

[3]Department of Pathology, The Ohio State University, Columbus, Ohio

[4]Center for Biostatistics, The Ohio State University, Columbus, Ohio

[5]Comprehensive Cancer Center, The Ohio State University, Columbus, Ohio

[#] These authors contributed equally to this work.

Abstract

Endocrine resistance is a major challenge in the management of estrogen receptor (ER)-positive breast cancers. Although multiple mechanisms leading to endocrine resistance have been proposed, the poor outcome of patients developing resistance to endocrine therapy warrants additional studies. Here we show that noncanonical Hedgehog (Hh) signaling is an alternative growth promoting mechanism that is activated in tamoxifen-resistant tumors. Importantly, phosphoinositide 3-kinase inhibitor/protein kinase B (PI3K/AKT) pathway plays a key role in regulating Hh signaling by protecting key components of this pathway from proteasomal degradation. The levels of Hh-signaling molecules SMO and GLI1 and the targets were significantly elevated in tamoxifen-resistant MCF-7 cells and T47D cells. Serial passage of the resistant cells in mice resulted in aggressive tumors that metastasized to distant organs with concurrent increases in Hh marker expression and epithelial mesenchymal transition. RNAi-mediated depletion of SMO or GLI1 in the resistant cells resulted in reduced proliferation, clonogenic survival and delayed G_1–S transition. Notably, treatment of resistant cells with PI3K inhibitors decreased SMO and GLI1 protein levels and activity that was rescued upon blocking

Corresponding Author: Sarmila Majumder, 511 Biomedical Research Tower, 450 West 12th Avenue, Columbus, OH 43210. Phone: 614-292-0103; Fax: 614-292-6356; Sarmila.majumder@osumc.edu.

Note: Supplementary data for this article are available at Cancer Research Online (http://cancerres.aacrjournals.org/).

Disclosure of Potential Conflicts of Interest
No potential conflicts of interest were disclosed.

Authors' Contributions
Conception and design: B. Ramaswamy, S. Majumder
Development of methodology: Y. Lu, K. Teng, G. J. Nuovo, S. Majumder
Acquisition of data (provided animals, acquired and managed patients, provided facilities, etc.): B. Ramaswamy, Y. Lu, K. Teng, G. J. Nuovo, C. L. Shapiro
Analysis and interpretation of data (e.g., statistical analysis, biostatistics, computational analysis): B. Ramaswamy, Y. Lu, K. Teng, G. J. Nuovo, X. Li, S. Majumder
Writing, review, and/or revision of the manuscript: B. Ramaswamy, Y. Lu, X. Li, C. L. Shapiro, S. Majumder
Administrative, technical, or material support (i.e., reporting or organizing data, constructing databases): K. Teng, S. Majumder
Study supervision: B. Ramaswamy, S. Majumder

GSK3β and proteasomal degradation. Furthermore, treatment of tamoxifen-resistant xenografts with anti-Hh compound GDC-0449 blocked tumor growth in mice. Importantly, high GLI1 expression correlated inversely with disease-free and overall survival in a cohort of 315 patients with breast cancer. In summary, our results describe a signaling event linking PI3K/AKT pathway with Hh signaling that promotes tamoxifen resistance. Targeting Hh pathway alone or in combination with PI3K/AKT pathway could therefore be a novel therapeutic option in treating endocrine-resistant breast cancer.

Introduction

Breast cancer is the most common cause of cancer-related death in women globally. Death rates from breast cancer have been steadily decreasing since 1990, which is attributed largely to better screening methods and improved treatment options. Perhaps, the major breakthrough in the treatment of breast cancer was the development of targeted therapies with drugs such as tamoxifen, a selective estrogen receptor (ER) modulator that blocks estrogen signaling. This therapeutic approach has been successfully used to treat approximately two-thirds of ER-positive breast cancers resulting in 50% improvement in disease-free survival (1). A recurring problem is, however, the development of acquired resistance to ER-targeted therapies in about 30% to 40% of the woman treated with tamoxifen for 5 years. Several signaling pathways are implicated in tamoxifen resistance including PI3K/mTOR/Akt, HER2/ERB, and insulin-like growth factor receptor (IGF-R) pathways (2–6). A few agents targeting these pathways in hormone-refractory breast cancers are in clinical trials (5, 7). To date, however, there is no approved targeted therapy to improve outcomes in hormone-refractory breast cancers without resorting to chemotherapy.

The hedgehog (Hh) signaling pathway is highly conserved and plays a crucial role in vertebrate embryogenesis (8). The Hh ligands (SHH, IHH, and DHH) bind to the cell surface receptor Patched (PTCH), which otherwise inhibits the activity of the transmembrane receptor like protein Smoothened (SMO). Release of SMO from PTCH-mediated repression results in posttranslational processing of the GLI (glioma-associated oncogene homolog)–zinc-finger transcription factors. Three mammalian GLI proteins are known to exist out of which GLI1 and GLI2 usually act as transcriptional activators and GLI3 acts as a transcriptional repressor (9). Aberrant activation of the Hh pathway has been reported in several cancers including basal cell carcinomas, medulloblastomas, pancreatic adenocarcinomas, and glioblastomas (10–12). Several lines of evidence point toward involvement of Hh signaling in breast carcinogenesis, and hence provide an attractive, rational therapeutic target in treating this cancer (13).

Mice with heterozygous disruption of *Ptch1* showed marked abnormalities in mammary glands resembling ductal dysplasias and hyperplasias (14). Further, expression of activated human SMO (SmoM2) in mouse mammary epithelium led to increased proliferation, altered differentiation, and ductal dysplasias distinct from those caused by Ptch1 heterozygosity (15). Hh signaling is also activated in human mammary stem/progenitor cells and is downregulated upon cell differentiation (16). It may also play a part in breast cancer progression through its role in communication between epithelial and stromal compartments (17, 18). Furthermore, higher expression ofSHH in breast tumors was significantly associated with increased risk of metastasis and breast cancer-specific death (19).

Here we present *in vitro* and *in vivo* data showing the dependence of endocrine-resistant breast cancer cells on activated Hh signaling for growth and the mechanism for this activation. In addition, we also present data supporting the clinical use of Hh inhibitors in endocrine-resistant tumors.

Materials and Methods

Reagents

Inhibitors of PI3K (LY294002 and Wortmannin) and glycogen synthase kinase-3 (GSK-3; LiCl) were from Sigma. AKT inhibitor [1L-6-hydroxymethyl-chiro-inositol 2-(R)-2-O-methyl-3-O-octadecylcarbonate] was from EMD Biosciences. GDC-0449 was synthesized at the Pharmacology core facility of The Ohio State University, following published protocol (20). MISSION siRNA universal negative Control and siRNA to SMO and GLI1 were from Sigma.

Cell culture and tissue procurement

Tamoxifen-sensitive MCF7 cells and OHTR100 cells (resistant to 100 nmol/L tamoxifen) were obtained from Dr. Kenneth P. Nephew (Indiana University, Bloomington, Indiana) and maintained as described (21). OHTR100 cells were further cultured in 500 nmol/L 4-hydroxy tamoxifen (4-OHT) for 1 month to obtain the OHTR500 cells, followed by exposure to 1,000 nmol/L tamoxifen to obtain the OHTR1000 cells. T47D cells were obtained from American Type Culture Collection and maintained as instructed. Cell lines were not passaged longer than 6 months after receipt. Primary human breast samples were obtained from the Stephanie Spielman Tissue Bank (protocol 2003C0036).

RT-PCR analysis

cDNA was synthesized from DNase-treated total RNA and gene expression (SHH, SMO, GLI1, GLI2, and GLI3) was measured in quadruplicate using Taqman assays (Applied Biosystems). Expression of SNAIL, MYC, and BMI1 was measured using Sybr Green chemistry.

Western blot analysis

Whole cell extracts were prepared in the cell lysis buffer, followed by immunoblotting as described (22). Protein expression was quantified by the ImageJ Software (http://rsbweb.nih.gov/ij/).

Plasmids, transfections, and luciferase assay

Dr. Hiroshi Sasaki gifted a 8 × 3′Gli BS-δ5′-Luc plasmid (9). pLKO.1-shGLI1 plasmid was from Thermo Scientific. Cells (1.6×10^5/well) seeded in a 24-well plate were transfected for 6 hours with 8 × 3′Gli-BS-δ5′-Luc plasmid and pRLTK (internal control, Promega) using Lipofectamine 2000 (Invitrogen). Luciferase activity was measured using the Dual-Luciferase Assay System (Promega) after 48 hours of transfection. OHTR2nd cells were routinely used to study the mechanism of Hh pathway activation as this pathway is highly active in these cells.

Cell proliferation assay

Cells (4,000/well) seeded in 96-well plates were serum starved overnight and treated with 5 μmol/L tamoxifen for 72 hours. Cell proliferation was monitored using a MTT assay kit (Roche Molecular Biochemicals), following company's protocol.

Colony formation assay

The assay was conducted as described previously (23). Briefly, exponentially growing cells (500/well) in 6-well plates were treated with indicated concentrations of tamoxifen for 2 weeks. When colonies were readily visible (>50 cells/colony) they were fixed in methanol

and stained with 1% crystal violet solution. The colony number was quantified using the Alpha-View Software 3.1 (FluorChem Q).

Flow cytometric analysis

Trypsinized cells were fixed in ice-cold 70% ethanol and stored at −20°C. Before analysis, samples were washed in phosphate-buffered saline (PBS) and stained with 5.0 μg/mL propidium iodide in PBS containing 0.2 mg/mL RNaseA. The single-cell suspensions were analyzed by a FACSCalibur (BD Biosciences) using the Cell Quest Software, and cell-cycle distribution was assessed using the ModFit program (Verity Software House).

Mouse mammary tumor induction and drug treatment

Cells (5×10^6) were grafted in mammary fat pads of ovariectomized Balb/c nude mice (Charles River Laboratory) with subcutaneous (s.c) supplementation of 0.72 mg 17-β-estradiol pellet (Innovative Research of America). When the tumor reached approximately 100 mm^3, the mice received 5 mg, 60-day sustained release pellet of tamoxifen citrate (Innovative Research of America) subcutaneously. Freshly formulated suspension of GDC-0449, in 0.5% methylcellulaose, 0.1% Tween-80 (24) was administered orally at 100 mg/kg body weight (25), twice daily for 10 days. Length (L) and width (W) of the tumors were measured twice a week, and tumor volume was calculated using the formula $\pi L W^2/6$, as previously described (26).At least 5 animals per group were used in each experiment.

Immunohistochemical analysis

The expression of Hh markers in primary tumors was determined by immunohistochemistry using Benchmark LT automated system (Ventana Medical Systems; ref. 27). The positive and negative controls are expressing and nonexpressing tissues, respectively, with and without primary antibody. Expressions of the markers were scored on the basis of percentage-positive cells and intensity of the staining by two independent pathologists. In case of discrepancy, an independent reader was consulted and consensus was obtained. A score of 10% or more was considered positive. All clinical follow-up was derived from the James Tumor Registry, OSU with a median follow-up of 96 months (0.93, 139.1 months).

Statistical analysis

The standard 2-tailed Student t-test was used for 2 data sets. ANOVA followed by Bonferroni/Dunn posttests were used for data sets with multiple groups using Prism 5.0 (GraphPad Software Inc.). Two-sided P values of equal or less than 0.05 were deemed to be statistically significant. Representative data from 2 to 3 reproducible experiments are presented, where error bars represent standard deviation (SD) or standard error of the mean (SEM) in animal experiments. For patient data, summary statistics were calculated to show patient characteristics. Fisher's exact test was used to evaluate the association between 2 categorical variables, such as 2 Hh markers expression levels (high vs. low for both). Staining score of 10% or more was considered high as mentioned in the methodology section. Survival analysis was conducted to assess the impact of Hh marker expression and other known clinical prognostic factors (age at diagnosis, tumor grade, breast cancer subtypes, and nodal status) on disease-free and overall survival. Survival curves were estimated by Kaplan–Meier plots for a dichotomized variable and compared by the log-rank test. Variables with a P value less than 0.05 in the univariate Cox regression analysis were further examined in multivariate Cox regression models. Proportional hazard assumption was checked during the modeling process. Upon significant violation of the assumption, stratified Cox models were utilized by including the predictor as a stratification factor. The covariate adjusted hazard ratio (HR) and the 95% confidence interval (CI) for the Hh marker of interest was reported on the basis of thefinal model. The log-rank test was used to test the

Hh marker's effect on clinical outcome in patients with node positive and ER positive breast cancer. All patient data analyses were conducted using SAS 9.1 statistical software (SAS institute Inc).

Results

Hedgehog signaling pathway is aberrantly activated in tamoxifen-resistant cell lines

As a first step to determine if Hh signaling pathway is activated in tamoxifen-resistant breast cancer cells, the expression of genes encoding Hh pathway components and their protein levels were analyzed in tamoxifen-sensitive and tamoxifen-resistant breast cancer cell lines. The model cell lines used for this study were tamoxifen-sensitive MCF7 cells and a panel of MCF7 cells that are resistant to increasing concentration of 4-OHT (OHTR100, OHTR500, and OHTR1000; Supplementary Fig. S1A). About 20% decrease in cell growth was observed when the resistant cells were exposed to 2.5 and 5 μmol/L tamoxifen (Supplementary Fig. S1B), showing the resistance. Real-time RT-PCR revealed a consistent increase in expression of *SHH*, *SMO*, and *GLI1* in the OHTR cell panel that correlated with the level of tamoxifen resistance (Fig 1A), whereas *GLI2* and *GLI3* expression were not significantly changed (data not shown). There was no marked change in the amount of PTCH RNA in OHTR cells (Fig. 1A). Western analysis of the Hh signaling molecules confirmed a marked increase in the protein levels of SMO and GLI1 in the resistant cells, whereas SHH was not detected (Fig. 1B). The protein levels of PTCH (Fig. 1B), GLI2, and GLI3 remain unaltered (Supplementary Fig. S1C).

It is known that T47D cells are relatively more resistant to tamoxifen compared with other ER-positive cell lines (28). Consistent with this finding, the level of SMO and GLI1 proteins were significantly higher in the T47D cells compared with tamoxifen-sensitive cell lines MCF7 and BT474 (Fig.1C). In contrast, the expression of PTCH was comparable in all cell lines.

Because GLI1 is a transcription factor, we tested the functional significance of increased expression of this gene in the tamoxifen-sensitive and tamoxifen-resistant cells, using a GLI responsive luciferase reporter vector (9). Analysis of luciferase expression revealed a 6- to 7-fold increase in promoter activity in the OHTR cells compared with the MCF7 cells ($P < 0.001$; Fig. 1D), showing that transcriptional activity of GLI1 is comparatively higher in the tamoxifen-resistant cells. Furthermore, depletion of GLI1 using GLI1-specific shRNA led to about 65% ($P < 0.01$) decrease in GLI-driven promoter activity (Fig. 1E).

We next analyzed the expression of the Hh target genes in the MCF-7 and OHTR cell lines. The expression of *SNAIL*, *BMI1*, and *MYC* mRNA in tamoxifen-resistant cells were significantly increased (2.5- to 4-fold; Fig. 1F). MYC and BMI1 protein levels were also found to be markedly higher (~5-fold and >17-fold, respectively) in the tamoxifen-resistant cells, and directly correlated with higher levels of tamoxifen resistance (Fig. 1G).

Tamoxifen-resistant xenografts in mouse mammary gland undergo micro-metastasis with concurrent increase in Hedgehog signaling

To study further the relationship between activated Hh signaling and tamoxifen resistance of breast tumors *in vivo*, tumor xenografts were established in Balb/c nude mice using OHTR100 cells. The tumors were serially passaged in mice treated with tamoxifen and a consistent increase in the growth rate of the tumors was observed after each passage (Fig. 2A). Microscopic analysis of hematoxylin and eosin stain (H&E) sections from the liver and lung of mice after the third passage revealed metastatic lesions in both tissues, indicating that the tamoxifen resistant cells acquired a more aggressive phenotype after *in vivo* passage (Fig. 2B). After each *in vivo* passage, cells were isolated from the macro-dissected tumors

and cultured *in vitro* (OHTR1st, 2nd, and 3rd). Comparison of the morphology of these cells revealed the acquisition of a more mesenchymal phenotype in the OHTR3rd cells (Fig. 2C). Consistent with this finding, we observed increased expression of vimentin, decreased expression of E-cadherin (Fig. 2D) and increased mammosphere formation (Supplementary Fig. S2A and B) in *in vivo* passaged cells. The expression of SMO and GLI1 increased after successive passages and were significantly higher (~3-fold) in the cells derived after the second and third passage in the mice (Fig. 2E). Similar increases in expression of the GLI1 target genes *MYC* were also observed (Fig.2E). Immunocytochemical analysis revealed a marked increase in SMO, GLI1, and BMI1 in tamoxifen-resistant cells, with distinct nuclear localization of GLI1 (Fig. 2F). These data showed a strong relationship between acquisition of the aggressive phenotype of tamoxifen-resistant cells *in vivo* and the activation of Hh signaling in the resistant tumors.

Knockdown of Hh pathway components inhibits growth of tamoxifen-resistant cells

To determine the functional significance of Hh pathway in tamoxifen resistance, we depleted SMO and GLI1 from OHTR2nd cells using the respective siRNA pools (Fig. 3A). A 60% decrease in SMO and 30% decrease in GLI1 protein level was routinely observed in the siRNA-transfected cells (Fig 3A). Comparison of cell proliferation to the scrambled siRNA-transfected control cells revealed a 66% ($P < 0.001$) and 25% ($P < 0.001$) decrease in growth of SMO- and GLI1-depleted cells, respectively. In the presence of 1.0 μmol/L tamoxifen, the growth of SMO-depleted cells was further reduced by 25% ($P < 0.001$) and that of GLI1-depleted cells by an additional 12% ($P < 0.05$), whereas the growth of the control cells remained unaffected (Fig. 3B). When assessed for clonogenic growth, we observed a 30% ($P < 0.001$) decrease in colony formation upon depletion of both SMO and GLI1. In the presence of 1.0 and 2.0 μmol/L tamoxifen, the colony formation was reduced by approximately 50% ($P < 0.001$) and 85% ($P < 0.01$), respectively, when SMO or GLI1 was depleted compared with the tamoxifen-treated control cells (Fig. 3C). Cell cycle analysis revealed significant retention of GLI1-depleted cells in the G_1 phase both in the absence ($P < 0.001$) and presence of tamoxifen ($P < 0.001$) at 6 and 12 hours compared with the control cells (Fig. 3D). There was no increase in the sub-G_0 population or apoptosis (Supplementary Fig. S3A and B). Similar growth suppression and sensitization to tamoxifen were also observed in 2 independently derived GLI1 shRNA knockdown T47D clones (Supplementary Fig. S3C–E). These clones showed decreased growth in the presence of tamoxifen and, decreased colony formation.

Analysis of target gene expression in SMO-depleted OHTR2nd cells and GLI1-depleted T47D cells revealed a marked reduction in the MYC protein (45%, Fig. 3E) and RNA level in both the cell lines (OHTR: 60%, T47D: 63—75%, Fig. 3E and Supplementary Fig. S3F). Further, the expression of BMI1 and SNAIL were also significantly reduced in these cells (~50% and >75% respectively, Fig. 3E, Supplementary Fig. S3F) and GLI1-depleted OHTR cells (data not shown).

The PI3K/AKT pathway activates Hh signaling in tamoxifen-resistant breast cancer

To elucidate the mechanism underlying aberrant activation of Hh pathway in tamoxifen-resistant breast cancer, we first used the GLI-luciferase reporter to determine whether a SHH autocrine loop could account for pathway activation in resistant cell. While the GLI reporter was strongly activated in OHTR^{2nd} cells, addition of recombinant SHH ligand had no effect on luciferase activity in OHTR^{2nd} or MCF7 cells (Fig. 4A). The data suggested that a noncanonical pathway might function to activate Hh signaling components and contribute to tamoxifen resistance of these cells. To test this hypothesis, OHTR2nd cells were routinely used to study the mechanism of Hh pathway activation as this pathway is highly active in these cells.

We hypothesized that the PI3K/AKT pathway, known to be associated with poor patient outcome in endocrine-resistant breast tumors (29, 30) is involved in Hh pathway activation. Consistent with this hypothesis, treatment with 20 μmol/L LY294002, a specific inhibitor of PI3K, resulted in a 50% decrease in GLI-dependent luciferase activity in OHTR2nd cells, but not in MCF7 cells (Fig. 4B). Similar inhibition of the GLI-reporter was also observed when cells were treated with 500 nmol/L of Wortmanin (45%, $P < 0.05$) or 20 μmol/L of a specific AKT inhibitor [1L-6-hydroxymethyl-chiro-inositol-2-(R)-2-O-methyl-3-O-octadecylcarbonate; 46%, $P < 0.05$; Supplementary Fig. S4A]. The inhibition by LY294002 was rescued when the constitutively active PI3K subunit P110 or an activated form of AKT was ectopically expressed in these cells (Fig. 4C-D). Furthermore, when vectors expressing dominant negative versions of P110 or AKT were transfected in the OHTR^{2nd} cells, the luciferase activity decreased by more than 90% and 25%, respectively (Fig. 4E). Conversely, coexpression of a constitutively active form of P110 in MCF7 cells resulted in nearly 2-fold ($P < 0.01$) increase in GLI-reporter activity (Fig. 4F). A small but significant increase in reporter activity was also observed in MCF-7 cells forced to express constitutively active AKT (0.25-fold, P 0.045; Fig. 4F).

To explore a potential mechanism underlying the PI3K pathway-activated Hh signaling, SMO and GLI1 protein levels were measured in LY294002-treated OHTR2nd cells. These cells showed approximately 50% decrease in SMO protein levels compared with vehicle dimethyl sulfoxide (DMSO)-treated controls (Fig. 4G, left). A similar reduction in GLI1 level was also observed after treatment with LY294002 (Fig. 4G, right).

GSK3β is a serine-threonine kinase that is negatively regulated by PI3K/AKT-mediated phosphorylation. We hypothesized that GSK3β-mediated phosphorylation of SMO and GLI1 facilitate ubiquitination and subsequent proteasomal degradation of these proteins in breast tumor cells. Activation of AKT in tamoxifen-resistant cells could thus rescue proteasomal degradation of these proteins by inhibiting GSK3β. Indeed, bioinformatics analysis using GPS software (31) revealed the presence of several potential phosphorylation motifs in SMO (Supplementary Table S1) and in GLI1 (Supplementary Table S2). To test this hypothesis, OHTR2nd cells were treated with LiCl, a potent and specific inhibitor of GSK3β, alone or with MG132 that inhibits proteasomal degradation. Western blot analysis showed approximately a 2-fold increase in SMO and GLI1 protein in the presence of LiCl or MG132 alone or in combination (Fig. 4H). Furthermore, stabilization of SMO and GLI1 by LiCl and MG132 was blocked when the cells were treated simultaneously with the PI3K inhibitor (Fig. 4I and Supplementary Fig. S4B).

These data showed that GSK3β-mediated phosphorylation can indeed lead to proteasomal degradation of these two proteins and that the PI3K/AKT pathway plays a key role in stabilizing these signaling molecules thereby promoting activation of the Hh pathway in the resistant cells.

GDC-0449, a small molecule inhibitor of SMO inhibits tamoxifen-resistant cell growth both *in vitro* and *in vivo*

GDC-0449, a small molecule inhibitor of SMO is in clinical trials for several cancers with activated Hh pathway (http.clinicaltrials.gov), including one in breast cancer. We used this compound to determine if the growth of tamoxifen-resistant cells could be suppressed with this inhibitor alone or in combination with tamoxifen using both *in vivo* and *in vitro* assays (Fig. 5A-D). For *in vivo* assays, xenografts were established in athymic nude mice with OHTR2nd cells. After implanted tumors reached approximately 100 mm^3 in size, the mice were randomized in 4 groups: vehicle, tamoxifen alone, GDC-0449 alone, and both tamoxifen and GDC-0449. The mice were treated for 10 consecutive days and the tumor growth was monitored for an additional 2 weeks (Fig. 5A). While the control group tumor

reached 500 mm^3 in volume at the endpoint of the assay, the GDC-0449-treated tumors failed to grow. In fact, the tumors shrank by approximately 50% from the day of treatment by day 24. Treatment with tamoxifen alone caused a 2.5-fold reduction in tumor size compared with the control group, whereas the combination of both tamoxifen and GDC-0449 had no additional effect compared with GDC-0449 alone (Fig. 5B and C).

In *in vitro* studies, GDC -0449 alone inhibited the growth of OHTR2nd and T47D cells by about 50% ($P < 0.05$). Importantly, the combination of GDC-0449 with tamoxifen suppressed growth of OHTR2nd and T47D cells ($P < 0.001$, Fig. 5D and E) almost completely. Similar observations were also recorded with all other OHTR cell lines (data not shown). Growth of parental MCF7 cells was inhibited by approximately 15% when treated with GDC-0449 (data not shown). These data suggest that GDC-0449 alone could be a targeted therapy for patients with ER+ breast cancer who failed to respond to tamoxifen as the first line of therapy.

GLI1 expression in primary human breast tumors correlates inversely with disease-free survival and overall survival

To extend this key observation regarding the role of GLI1 in breast cancer to patient survival, tissue microarrays containing tissue cores representing 315 invasive breast cancers were stained for Hh markers. The tumors were obtained through a tissue banking protocol (OSU2009C009A) where patients with newly diagnosed breast cancer were consented to have their tumors stored for future research purposes and for long-term clinical follow-up. The median follow-up was 96 months. The clinicopathologic characteristics of the tumors are listed in Table 1. The expression of GLI1 and BMI1 are presented in Fig. 6A. Epithelial and stromal GLI1 expression was observed in 69% and 47% of the tumors, respectively. Epithelial Gl1 expression positively correlated with epithelial and stromal BMI1 expression ($P < 001$). A significant correlation was found between increased epithelial GLI1 expression and lymph node status ($P = 0.014$) but no significant association existed between GLI1 expression and ER ($P = 0.31$), PR (P 0.33), HER2 ($P = 0.42$) status and grade ($P = 1$) of the tumor.

To establish a potential relationship between GLI1 over-expression and clinical outcomes, we first conducted univariate survival probability analysis. Univariate survival analysis showed that the following factors were associated with shorter disease-free survival: high-epithelial GLI1 expression, ER-negative status, lymph node-positive status, higher tumor grade, and Her2-positive tumors (Table 2). No significant violation of proportionality was detected for these variables. Multivariate survival analysis showed that high epithelial GLI1 expression was independently associated with shorter DFS [$P = 0.0375$, HR 1.954 (1.039, 3.671)] when controlled for ER [$P = 0.0008$, HR 0.397 (0.231, 0.682)], HER2 [P 0.0241, HR 1.908 (1.088, = 3.346)], and nodal status [P 0.0057= = HR 2.108 (1.242, 3.576); Fig. 6B]. When analyzing this data on the basis of molecular subtypes, among ER-positive tumors ($N = 230$), epithelial GLI1 expression correlated with worse DFS in patients with node-positive disease only ($P < 0.01$; Fig. 6C). For overall survival, univariate survival analysis results were presented in Table 3. Multivariate analysis selected the final model in which grade and ER were stratified and still showed a significant GLI effect [$P = 0.014$, HR 2.156 (1.17, 3.98)] after adjusting for nodal status (Fig. 6D).

Furthermore, we asked the question whether among patients that received tamoxifen as part of their adjuvant therapy, if high GLI1 expression resulted in worse DFS. Among the 98 patients with ER positive breast cancer, who received tamoxifen as part of their adjuvant therapy, there were only a total of 20 events in 10 years of follow-up and no statistically significant difference was seen between the groups with high or low expression of GLI1.

Considering the overall excellent prognosis in this subset of patients, a larger sample size is needed to identify a statistically significant difference in clinical outcomes.

Discussion

We show here for the first time the efficacy of targeting Hh pathway using a small molecule SMO inhibitor in improving outcomes in tamoxifen-resistant tumors. Acquired resistance to endocrine therapy such as tamoxifen is a major clinical concern in the management of patients with hormone-receptor-positive breast cancer, which is clearly a complex phenomenon involving multiple pathways (32–36). Receptor tyrosine-kinases have been frequently targeted to overcome endocrine resistance in the past. We have presented here compelling data using multiple approaches to show the role of Hh signaling pathway in inducing tamoxifen-resistance, and the mechanism of its activation.

Furthermore, we have showed a significant correlation between activation of Hh signaling in primary tumors ($n = 315$), and disease outcomes, confirming the negative prognostic effect of high GLI1 expression on DFS and OS. Although GLI1 expression did not correlate with a particular molecular subtype, among ER positive, node positive tumors DFS was worse in tumors with high GLI1expression. Hence the overall association of Hh activation and poor outcome in breast cancer signifies that activation of this pathway facilitates tumor growth and progression, supporting recently reported association of increased Hh ligand expression with increased risk of metastasis and breast cancer-specific death (19).

Our *in vivo* study revealed that blocking SMO with GDC-0449 alone could effectively suppress the tamoxifen-resistant xenografts in mice. Unlike our *in vitro* studies, addition of tamoxifen to GDC-0449 had no further benefit, which could be because of the high dosage of GDC-0449 used in the *in vivo* studies, or the tamoxifen concentrations achieved in the tumor may be lower depending on its conversion to active metabolite *in vivo*. Using monoclonal antibody 5E1 to Hh ligand (Shh) O'Toole and colleagues showed metastases reduction in animal models of breast cancer (19). Our data is unique in showing that targeting the noncanonical Hh pathway specifically in ER-positive breast cancers that are tamoxifen resistant using a clinically available Hh inhibitor (GDC-0449) improves outcomes. GDC-0449 (vismodegib) is a well tolerated, orally bioavailable compound that is approved for the management of metastatic or locally advanced basal cell carcinomas and being explored in other cancers (http.clinicaltrials.gov). Our work indicates that patients who developed resistance to tamoxifen, GDC-0049 alone will be effective in treating recurrent tumors and therefore designing appropriate clinical trials is warranted. It will be interesting to determine if resistance to other endocrine therapies such as aromatase inhibitors results in Hh pathway activation, which we plan to pursue in the future.

One of the major challenges in treating a drug-resistant tumor is the complex networking pathways that are involved in the cross-talk between the distinct signaling pathways. The PI3K/AKT pathway is one of many pathways that contribute to endocrine resistance (37). Activation of the PI3K/AKT and the p42/44 mitogen-activated protein kinase pathways by receptors such as EGFR and IGF1-R suppresses the expression of ER and PR (29, 38–42) and therefore, reduce estrogen dependence. Our work clearly shows cross-talk between PI3K/AKT and Hh pathway, and provides an additional mechanism for PI3K/AKT-mediated endocrine resistance. Importantly, we showed that increased activity of PI3K/AKT activity could stabilize SMO and GLI1 protein by suppressing GSK3β-mediated phosphorylation and proteasomal degradation, leading to noncanonical Hh pathway activation. Although a previous study reported cross-talk between PI3K/AKT and Hh pathway, it is in NIH3T3 cells through activation of Hh ligands (43). Our data suggests a

rationale for combined targeting of PI3K/AKT and Hh pathway to effectively overcome endocrine resistance.

In summary, there is still an urgency in designing targeted therapies to overcome endocrine resistance. Our study presents a potential therapeutic option to overcome such resistance and a clinical trial targeting Hh pathway in advanced hormone-refractory breast cancer is warranted and is currently being pursued. Further, our finding underscores the importance of PI3K pathway in activating Hh pathway and provides the rationale for combinatorial targeted therapy in breast cancer.

Supplementary Material

Refer to Web version on PubMed Central for supplementary material.

Acknowledgments

We thank Dr. Michael Ostrowski for critical reading of the manuscript and editorial suggestions and Drs. Samson T. Jacob, Miguel A. Villalona, Gustavo Leone, Guido Marcucci, and Cynthia Timmers for critically reading the manuscript.We thank Dr. Hiroshi Sasaki for kindly providing the GliBS-δ5′-Lucplasmid and Dr. Kristian Helin for providing the PI3K and AKT expression vectors. We also thank Satavisha Roy and Thomas Kaffenberger for technical help.

Grant Support

This work was supported by National Institutes of Health Grant CA137567 to S. Majumder, CA133250-01 to B. Ramaswamy, Pelotonia Idea grant to S. Majumder and B. Ramaswamy, and Experimental Therapeutics OSU internal grant to S. Majumder and B. Ramaswamy.

References

1. Early Breast Cancer Trialists' Collaborative Group. Tamoxifen for early breast cancer: an overview of the randomised trials. Lancet. 1998; 351:1451–67. [PubMed: 9605801]
2. Arpino G, Green SJ, Allred DC, Lew D, Martino S, Osborne CK, et al. HER-2 amplification, HER-1 expression, and tamoxifen response in estrogen receptor-positive metastatic breast cancer: a southwest oncology group study. Clin Cancer Res. 2004; 10:5670–6. [PubMed: 15355892]
3. Campbell RA, Bhat-Nakshatri P, Patel NM, Constantinidou D, Ali S, Nakshatri H. Phosphatidylinositol 3-kinase/AKT-mediated activation of estrogen receptor alpha: a new model for anti-estrogen resistance. J Biol Chem. 2001; 276:9817–24. [PubMed: 11139588]
4. Ellis MJ, Tao Y, Young O, White S, Proia AD, Murray J, et al. Estrogen-independent proliferation is present in estrogen-receptor HER2-positive primary breast cancer after neoadjuvant letrozole. J Clin Oncol. 2006; 24:3019–25. [PubMed: 16754938]
5. Miller TW, Perez-Torres M, Narasanna A, Guix M, Stål O, Pérez-Tenorio G, et al. Loss of Phosphatase and Tensin homologue deleted on chromosome 10 engages ErbB3 and insulin-like growth factor-I receptor signaling to promote antiestrogen resistance in breast cancer. Cancer Res. 2009; 69:4192–201. [PubMed: 19435893]
6. Shou J, Massarweh S, Osborne CK, Wakeling AE, Ali S, Weiss H, et al. Mechanisms of tamoxifen resistance: increased estrogen receptor-HER2/neu cross-talk in ER/HER2-positive breast cancer. J Natl Cancer Inst. 2004; 96:926–35. [PubMed: 15199112]
7. Baselga J, Campone M, Piccart M, Burris HA III, Rugo HS, Sahmoud T, et al. Everolimus in postmenopausal hormone-receptor-positive advanced breast cancer. N Engl J Med. 2011; 366:520–9. [PubMed: 22149876]
8. Varjosalo M, Taipale J. Hedgehog: functions and mechanisms. Genes Dev. 2008; 22:2454–72. [PubMed: 18794343]
9. Sasaki H, Nishizaki Y, Hui C, Nakafuku M, Kondoh H. Regulation of Gli2 and Gli3 activities by an amino-terminal repression domain: implication of Gli2 and Gli3 as primary mediators of Shh signaling. Development. 1999; 126:3915–24. [PubMed: 10433919]

10. Hahn H, Wicking C, Zaphiropoulous PG, Gailani MR, Shanley S, Chidambaram A, et al. Mutations of the human homolog of Drosophila patched in the nevoid basal cell carcinoma syndrome. Cell. 1996; 85:841–51. [PubMed: 8681379]
11. Johnson RL, Rothman AL, Xie J, Goodrich LV, Bare JW, Bonifas JM, et al. Human homolog of patched, a candidate gene for the basal cell nevus syndrome. Science. 1996; 272:1668–71. [PubMed: 8658145]
12. Reifenberger J, Wolter M, Weber RG, Megahed M, Ruzicka T, Lichter P, et al. Missense mutations in SMOH in sporadic basal cell carcinomas of the skin and primitive neuroectodermal tumors of the central nervous system. Cancer Res. 1998; 58:1798–803. [PubMed: 9581815]
13. Hatsell S, Frost AR. Hedgehog signaling in mammary gland development and breast cancer. J Mammary Gland Biol Neoplasia. 2007; 12:163–73. [PubMed: 17623270]
14. Lewis MT, Ross S, Strickland PA, Sugnet CW, Jimenez E, Scott MP, et al. Defects in mouse mammary gland development caused by conditional haploinsufficiency of Patched-1. Development. 1999; 126:5181–93. [PubMed: 10529434]
15. Moraes RC, Zhang X, Harrington N, Fung JY, Wu MF, Hilsenbeck SG, et al. Constitutive activation of smoothened (SMO) in mammary glands of transgenic mice leads to increased proliferation, altered differentiation and ductal dysplasia. Development. 2007; 134:1231–42. [PubMed: 17287253]
16. Liu S, Dontu G, Mantle ID, Patel S, Ahn NS, Jackson KW, et al. Hedgehog signaling and Bmi-1 regulate self-renewal of normal and malignant human mammary stem cells. Cancer Res. 2006; 66:6063–71. [PubMed: 16778178]
17. Lamm ML, Catbagan WS, Laciak RJ, Barnett DH, Hebner CM, Gaffield W, et al. Sonic hedgehog activates mesenchymal Gli1 expression during prostate ductal bud formation. Dev Biol. 2002; 249:349–66. [PubMed: 12221011]
18. Fiaschi M, Rozell B, Bergstrom A, Toftgard R, Kleman MI. Targeted expression of GLI1 in the mammary gland disrupts pregnancy-induced maturation and causes lactation failure. J Biol Chem. 2007; 282:36090–101. [PubMed: 17928300]
19. O'Toole SA, Machalek DA, Shearer RF, Millar EK, Nair R, Schofield P, et al. Hedgehog overexpression is associated with stromal interactions and predicts for poor outcome in breast cancer. Cancer Res. 2011; 71:4002–14. [PubMed: 21632555]
20. Gunzer, JL.; Sutherlijn, DP.; Stanley, MS.; Bao, L.; Castendeo, G.; Lalonde, RL., et al. Pyridyl inhibitors of hedgehog signaling. 2009. WO/2009/126863, PCT/US2009/040165
21. Fan M, Yan PS, Hartman-Frey C, Chen L, Paik H, Oyer SL, et al. Diverse gene expression and DNA methylation profiles correlate with differential adaptation of breast cancer cells to the antiestrogens tamoxifen and fulvestrant. Cancer Res. 2006; 66:11954–66. [PubMed: 17178894]
22. Datta J, Kutay H, Nasser MW, Nuovo GJ, Wang B, Majumder S, et al. Methylation mediated silencing of MicroRNA-1 gene and its role in hepatocellular carcinogenesis. Cancer Res. 2008; 68:5049–58. [PubMed: 18593903]
23. Franken NA, Rodermond HM, Stap J, Haveman J, van Bree C. Clonogenic assay of cells in vitro. Nat Protoc. 2006; 1:2315–9. [PubMed: 17406473]
24. Dijkgraaf GJ, Alicke B, Weinmann L, Januario T, West K, Modrusan Z, et al. Small molecule inhibition of GDC-0449 refractory smoothened mutants and downstream mechanisms of drug resistance. Cancer Res. 2011; 71:435–44. [PubMed: 21123452]
25. Romer JT, Kimura H, Magdaleno S, Sasai K, Fuller C, Baines H, et al. Suppression of the Shh pathway using a small molecule inhibitor eliminates medulloblastoma in Ptc1(+/−)p53(−/−) mice. Cancer Cell. 2004; 6:229–40. [PubMed: 15380514]
26. Gupta GP, Nguyen DX, Chiang AC, Bos PD, Kim JY, Nadal C, et al. Mediators of vascular remodelling co-opted for sequential steps in lung metastasis. Nature. 2007; 446:765–70. [PubMed: 17429393]
27. Nasser MW, Datta J, Nuovo G, Kutay H, Motiwala T, Majumder S, et al. Down-regulation of micro-RNA-1 (miR-1) in lung cancer. Suppression of tumorigenic property of lung cancer cells and their sensitization to doxorubicin-induced apoptosis by miR-1. J Biol Chem. 2008; 283:33394–405. [PubMed: 18818206]

28. Horwitz KB, Mockus MB, Lessey BA. Variant T47D human breast cancer cells with high progesterone-receptor levels despite estrogen and antiestrogen resistance. Cell. 1982; 28:633–42. [PubMed: 7200400]
29. Creighton CJ, Fu X, Hennessy BT, Casa AJ, Zhang Y, Gonzalez-Angulo AM, et al. Proteomic and transcriptomic profiling reveals a link between the PI3K pathway and lower estrogen-receptor (ER) levels and activity in ER+ breast cancer. Breast Cancer Res. 2010; 12:R40. [PubMed: 20569503]
30. Kirkegaard T, Witton CJ, McGlynn LM, Tovey SM, Dunne B, Lyon A, et al. AKT activation predicts outcome in breast cancer patients treated with tamoxifen. J Pathol. 2005; 207:139–46. [PubMed: 16088978]
31. Xue Y, Zhou F, Zhu M, Ahmed K, Chen G, Yao X. GPS: a comprehensive www server for phosphorylation sites prediction. Nucleic Acids Res. 2005; 33:W184–7. [PubMed: 15980451]
32. Lu Y, Roy S, Nuovo G, Ramaswamy B, Miller T, Shapiro C, et al. AntimicroRNA-222 (anti-miR-222) and -181B suppress growth of tamoxifen-resistant xenografts in mouse by targeting TIMP3 protein and modulating mitogenic signal. J Biol Chem. 2011; 286:42292–302. [PubMed: 22009755]
33. Majumder S, Jacob ST. Emerging role of microRNAs in drug-resistant breast cancer. Gene Expr. 2011; 15:141–51. [PubMed: 22268296]
34. Musgrove EA, Sutherland RL. Biological determinants of endocrine resistance in breast cancer. Nat Rev Cancer. 2009; 9:631–43. [PubMed: 19701242]
35. Osborne CK, Schiff R. Mechanisms of endocrine resistance in breast cancer. Annu Rev Med. 2011; 62:233–47. [PubMed: 20887199]
36. Miller TE, Ghoshal K, Ramaswamy B, Roy S, Datta J, Shapiro CL, et al. MicroRNA-221/222 confers tamoxifen resistance in breast cancer by targeting p27Kip1. J Biol Chem. 2008; 283:29897–903. [PubMed: 18708351]
37. Clark AS, West K, Streicher S, Dennis PA. Constitutive and inducible Akt activity promotes resistance to chemotherapy, trastuzumab, or tamoxifen in breast cancer cells. Mol Cancer Ther. 2002; 1:707–17. [PubMed: 12479367]
38. Bayliss J, Hilger A, Vishnu P, Diehl K, El-Ashry D. Reversal of the estrogen receptor negative phenotype in breast cancer and restoration of antiestrogen response. Clin Cancer Res. 2007; 13:7029–36. [PubMed: 18056179]
39. Cui X, Zhang P, Deng W, Oesterreich S, Lu Y, Mills GB, et al. Insulin-like growth factor-I inhibits progesterone receptor expression in breast cancer cells via the phosphatidylinositol 3-kinase/Akt/mammalian target of rapamycin pathway: progesterone receptor as a potential indicator of growth factor activity in breast cancer. Mol Endocrinol. 2003; 17:575–88. [PubMed: 12554765]
40. Lopez-Tarruella S, Schiff R. The dynamics of estrogen receptor status in breast cancer: re-shaping the paradigm. Clin Cancer Res. 2007; 13:6921–5. [PubMed: 18056165]
41. Cui X, Schiff R, Arpino G, Osborne CK, Lee AV. Biology of progesterone receptor loss in breast cancer and its implications for endocrine therapy. J Clin Oncol. 2005; 23:7721–35. [PubMed: 16234531]
42. Guo S, Sonenshein GE. Forkhead box transcription factor FOXO3a regulates estrogen receptor alpha expression and is repressed by the Her-2/neu/phosphatidylinositol 3-kinase/Akt signaling pathway. Mol Cell Biol. 2004; 24:8681–90. [PubMed: 15367686]
43. Riobo NA, Lu K, Ai X, Haines GM, Emerson CP Jr. Phosphoinositide 3-kinase and Akt are essential for Sonic Hedgehog signaling. Proc Natl Acad Sci U S A. 2006; 103:4505–10. [PubMed: 16537363]

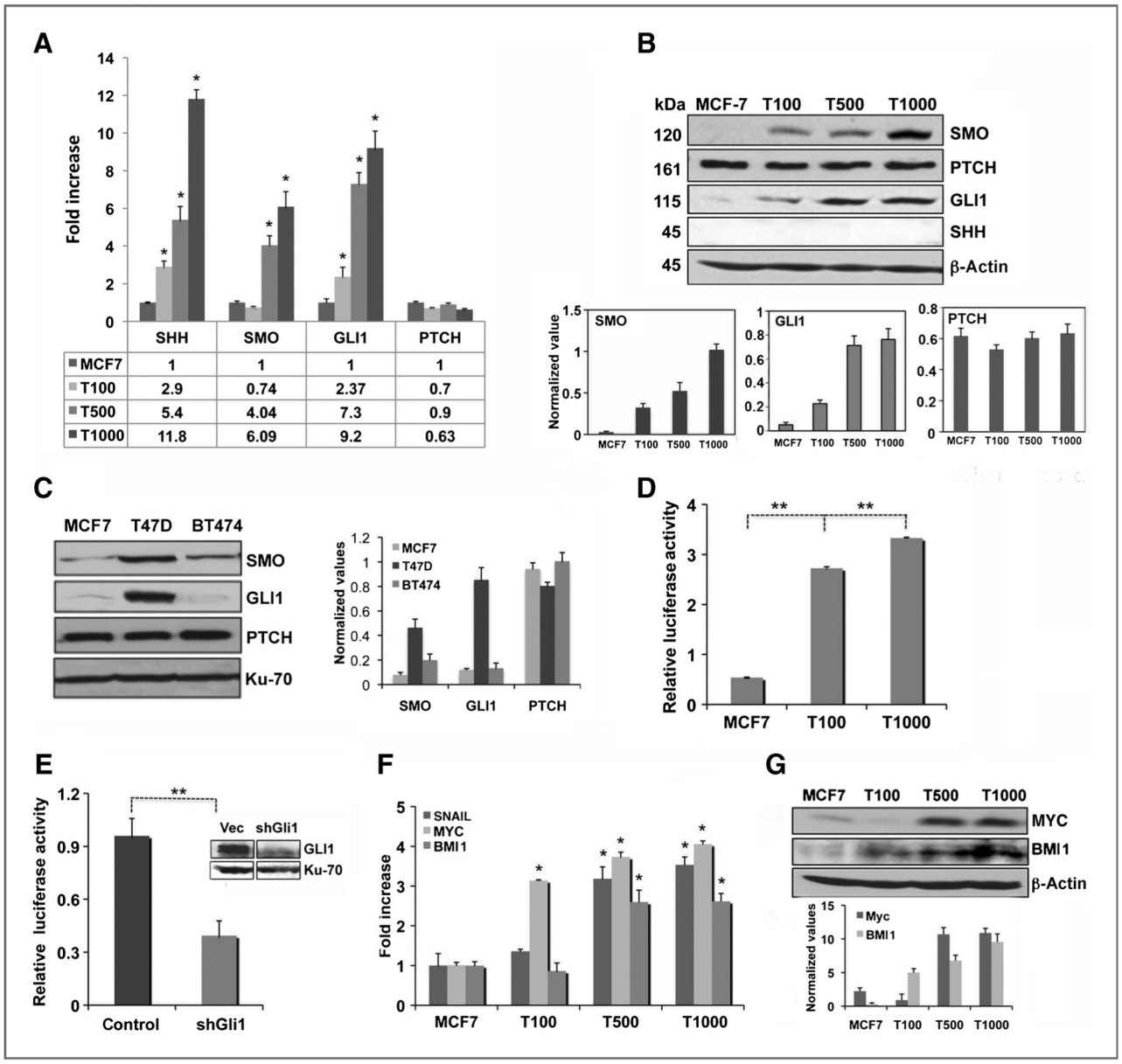

Figure 1.

Hh pathway is activated in tamoxifen-resistant breast cancer cells. A and B, real-time RT-PCR (A) and Western blot analysis of SHH, SMO, GLI1, and PTCH in MCF7 and OHTR cells (T100: OHTR100, T500: OHTR500, T1000: OHTR1000; B) quantified in the bar diagram. C, Western analysis and quantification of Hh markers in ER-positive cell lines. D and E, GLI-driven luciferase expression in MCF7 and OHTR cells (D) and after depletion of GLI1 in OHTR1000 cells (E). F and G, real-time RT-PCR (F) and Western analysis (G) of Hh target genes in MCF7 and OHTR cells quantified in the bar diagram.

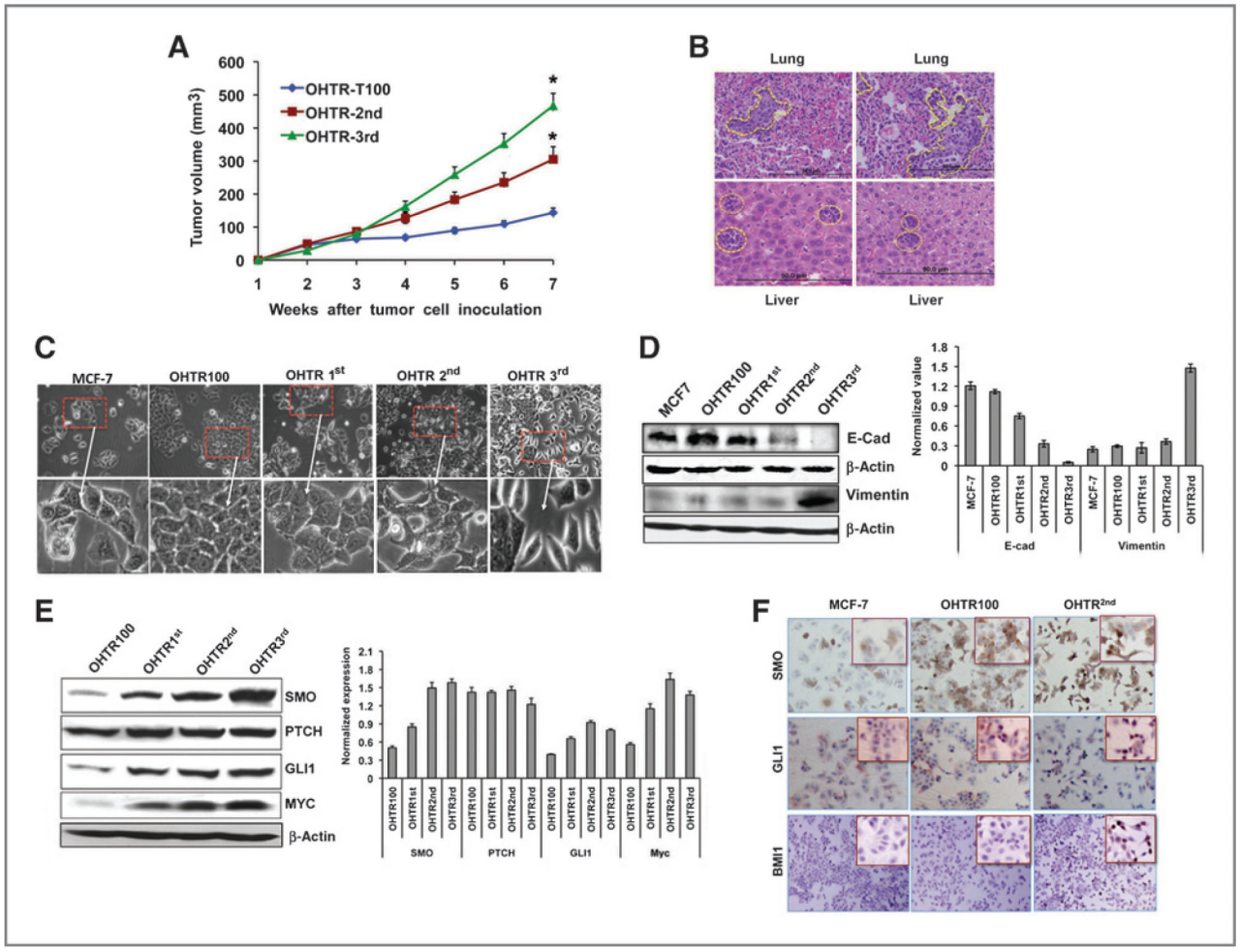

Figure 2.

Serial passage of tamoxifen-resistant xenografts in mice resulted in metastasis. A, growth curve of OHTR100 cells grafted in Balb/c nude mice ($n = 5$) at initial transplant (OHTR100), 2nd (OHTR2nd), and 3rd passage (OHTR3rd). B, H&E stain of lung and liver sections of mice-bearing OHTR3rd primary tumors. C, morphological changes acquired by OHTR100 cells upon serial passage in mice. D and E, Western analysis of E-cadherin and vimentin (D), Hh signaling and target proteins (E) in OHTR cells quantified in the bar diagram. F, immunocytochemical analysis of SMO, GLI, and BMI1, with insets at higher magnification.

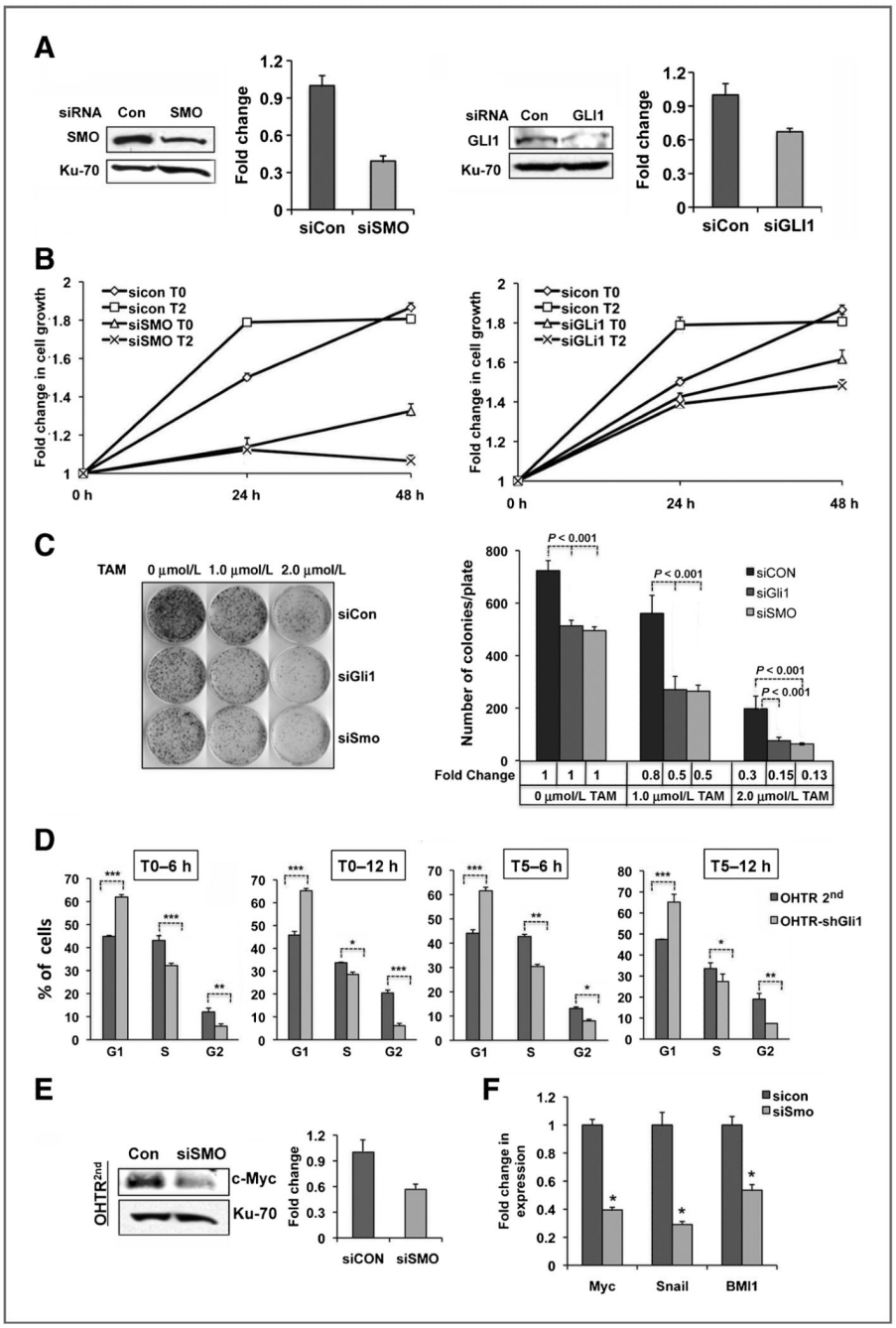

Figure 3.

SMO and GLI1 depletion inhibits tamoxifen-resistant cell growth. A, Western analysis of SMO and GLI1 knocked down OHTR2nd cells quantified in the bar diagram. B and C, cell proliferation assay (B) and clonogenic survival of SMO and GLI1 depleted cells in the absence (T0) and presence of 2 μmol/L tamoxifen (T2) quantified in the bar diagram (C). D, cell-cycle analysis of GLI1 depleted OHTR2nd cells without (T0) and with (T5) 5 μmol/L tamoxifen treatment. E and F, Western analysis of MYC (E) and real-time RT-PCR of MYC, SNAIL, and BMI1 (F) in SMO-depleted OHTR2nd cells.

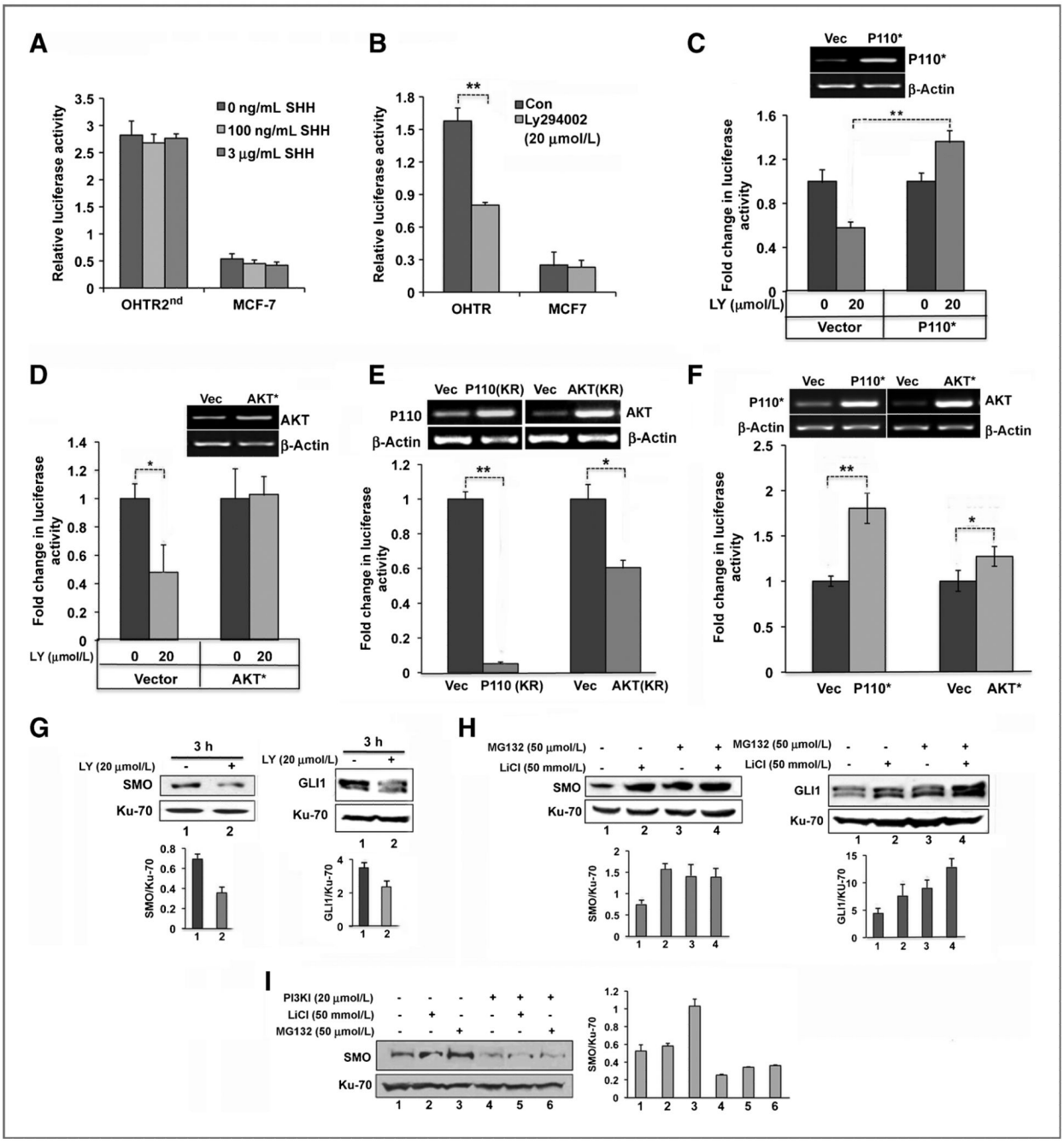

Figure 4.

PI3K/AKT pathway activates Hh signaling in tamoxifen-resistant cells. A, GLI- driven luciferase activity in OHTR2nd and MCF-7 cells treated with SHH. B, luciferase activity in OHTR2nd and MCF-7 cells treated with DMSO (Con) and 20 μmol/L LY294002 for 3 hours. C and D, luciferase activity in OHTR2nd cells overexpressing constitutively active P110 subunit of PI3K (P110*; C), and constitutively active AKT (AKT*) or the corresponding empty vectors (D), treated with 20 μmol/L LY294002 (LY). E and F, luciferase activity in OHTR2nd cells overexpressing dominant negative mutants of PI3K [P110(KR)] or AKT[AKT(KR); E] and in MCF-7 cells overexpressing P110* or AKT* (F). Ectopic expression of P110 and AKT mutants are shown in the inset. Western analysis of

SMO and GLI1 in OHTR2nd cells treated with 20 μmol/L LY294002 for 3 hours (G), 50 mmol/L LiCl for 6 hours alone or in combination of 50 μmol/L MG132 for the last 1 hour (H), and of SMO in OHTR2nd cells treated with 20 μmol/L LY294002 (LY) and/or 50 mmol/L LiCl for 6 hours, or 50 μmol/L MG132 for the last 1 hour (I), as indicated. Bar diagrams present quantified data.

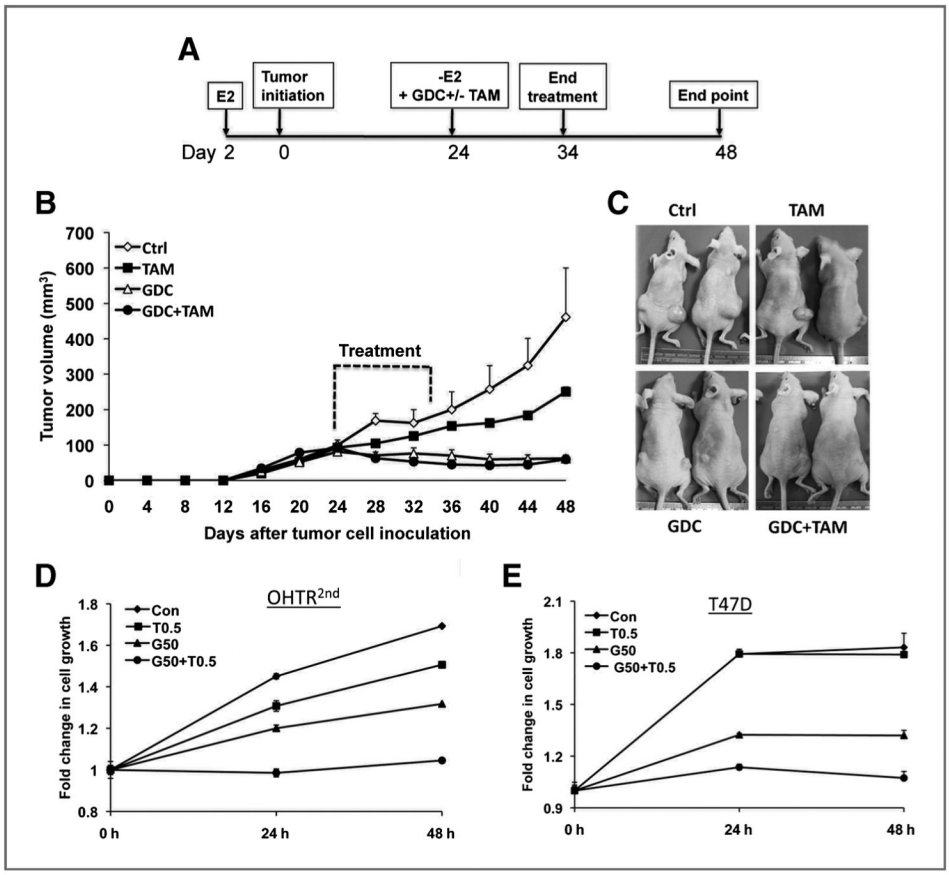

Figure 5.

GDC-0449 inhibits growth of OHTR cells *in vitro* and *in vivo*. A, timeline of tumor induction and GDC-0449/tamoxifen treatment in mice. B, comparison of growth curve of OHTR2nd cell-induced xenografts in mice treated with GDC-0449 alone or in combination with tamoxifen (n = 8). Average tumor volume ± SEM is plotted against time (in days). C, representative images of tumor bearing mice. D and E, growth of OHTR2nd (D) and T47D (E) cells in the presence of GDC-0449 (50 μmol/L, G_{50}) alone or in combination with tamoxifen (0.5 μmol/L, T0.5).

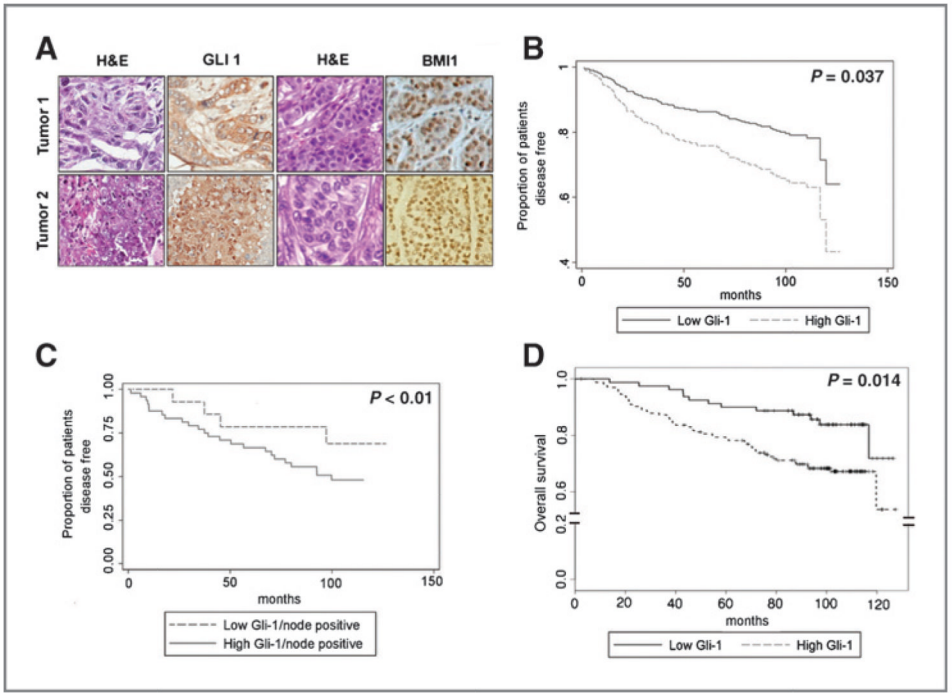

Figure 6.

GLI1 expression inversely correlates with DFS and OS in primary human breast tumors. A, representative pictures of breast tumors (H&E), GLI1, and BMI1 (immunohistochemistry). B, comparison of DFS amongst breast cancer patients with ER-positive tumors expressing high versus low GLI1. C, comparison of DFS amongst breast cancer patients with node positive, ER-positive tumors expressing high versus low GLI1. D, comparison of overall survival amongst patients with breast cancer tumors expressing high versus low GLI1.

Table 1

Clinicopathologic features of primary breast tumors (*N* = 315)

Patient Characteristics	***N* = 315**
Age	Median 54.5 (Range 20–92)
Race	
White	276 (88)
Black	35 (11)
Other	4(1)
Nodal status	
Positive	179 (57)
Negative	110 (35)
Unknown	26 (8)
Grade	
1	26 (8)
2	132 (42)
3	138 (44)
Unknown	19(6)
Estrogen receptor	
Positive	230 (73)
Negative	77 (24)
Unknown	8 (3)
Progesterone receptor	
Positive	206 (65)
Negative	99 (31)
Unknown	10(3)
Her2 neu status	
Positive	46 (15)
Indeterminate	26 (8)
Negative	161 (51)
Unknown	82 (26)

Table 2

Univariate analysis of factors impacting disease-free survival

Variable	Categorization	*N*	No. of events	*P*	HR (95%CI)
ER	Positive	230	73	<0.0001	0.391 (0.268–0.570)
	Negative	77	44		
PR	Positive	206	66	<0.0001	0.513 (0.354–0.743)
	Negative	99	50		
HER2	Positive	46	28	<0.0001	2.682 (1.701–4.230)
	Negative	187	58		
Nodal Status	Positive	110	55	<0.0001	2.654 (1.777–3.965)
	Negative	179	44		
Grade	G_3	138	60	0.0036	1.744 (1.193–2.548)
	G_1 and G_2	158	49		
Gli1 (epithelial)	Positive	200	83	0.0188	1.714 (1.088–2.701)
	Negative	89	24		

Table 3

Univariate survival analysis results for overall survival

Variable	Categorization	*N*	No. of events	*P*	HR (95%CI)
ER	Positive	230	65	<0.0001	0.428 (0.286–0.640)
	Negative	77	38		
PR	Positive	206	58	0.0013	0.526 (0.355–0.778)
	Negative	99	45		
HER2	Positive	46	26	0.0001	2.564 (1.592–4.129)
	Negative	187	51		
Nodal Status	Positive	110	50	<0.0001	2.983 (1.928–4.616)
	Negative	179	35		
Grade	G_3	138	40	0.002	1.907 (1.266–2.872)
	G_1 and G_2	158	55		
Gli1 (epithelial)	Positive	200	74	0.0055	2.076 (1.240–3.476)
	Negative	89	18		